DNS and LES of Turbulent Mixed Convection in the Minimal Flow Unit

Christian Kath and Claus Wagner

Abstract We performed Direct Numerical Simulations (DNS) and Large Eddy Simulation (LES) of turbulent mixed convection in the minimal flow unit. DNS of turbulent isothermal channel flow have been conducted to demonstrate the predictive capability of the second order accurate finite volume method we used. For the mixed convection case we obtained that the turbulence intensity increases due to bouyancy. Consequently, we reduced the spanwise width of the domain to show that turbulence can be sustained for mixed convection. Additionally, we launched a LES of mixed convection with the dynamic Smagorinsky model. The obtained LES results agree well with the corresponding DNS data.

1 Introduction

Research on wall-bounded turbulent flows is of considerable interest for many technological applications. It is also well known that the improved understanding of the transport phenomena closed to walls are of major importance for development of more sophisticated turbulence models. Various researchers summarized the experimental and numerical results of the last years on this subject in annual reviews. Most cited and with the largest impact on research on this subject were [1] and [2]. For the latest review on this topic the reader is referred to [3]. One major issue of these reviews are the development of coherent structures in the turbulent boundary layer. They are found in the viscous sublayer and buffer regions, where the bulk of the near-wall turbulence-production takes place [4]. In channel flows, these structures are alternating narrow streaks of fluid, which move at different speeds in streamwise direction [2]. Fluid from low-speed streaks is transported into the outer region while high-speed streaks receive fluid from the wall-distant zone.

C. Kath (✉) · C. Wagner
German Aerospace Center (DLR), Institute of Aerodynamics and Flow Technology, SCART, Göttingen, Germany
e-mail: christian.kath@dlr.de

A. Dillmann et al. (eds.), *New Results in Numerical and Experimental Fluid Mechanics IX*, Notes on Numerical Fluid Mechanics and Multidisciplinary Design 124,
DOI: 10.1007/978-3-319-03158-3_13,

In order to understand the complex interactions between coherent structures, Jiménez and Moin [5] (hereafter, JM) made several Direct Numerical Simulations (DNS) of turbulent channel flows in different narrow boxes. The idea was to isolate a single low-speed streak in a minimal channel. They have shown that there is minimal set of span- and streamwise widths, in which a turbulent boundary layer can be sustained. An interesting result was that the low-order statistics are in good agreement to those of DNS in the "full" channel in the regions close to the walls, although the minimal box seemed to be too small to adequately represent the turbulent flow in the region away from the wall. Furthermore, it turned out that there are active and passive periods, in which the turbulent boundary layer relaminarizes at one wall of the minimal channel. Indeed, this characteristic was not seen during experimental investigations so far. As they decreased the size of the spanwise width further, they observed the decay of the whole turbulent channel flow to a laminar state.

JM validated this simulations based on a study of the empirical correlation between the wall shear stress and the bulk velocity in channel flows by Dean [6]. The latter predicts that the size of the coherent structures decreases with increasing wall shear stress, while the turbulence production is considerbly enhanced. In this regard several reports (e. g. [7, 8]) point out that buoyancy severely modifies the shear stress in mixed convection. Thus, the primary objective of this work is to obtain and analyse results of turbulent mixed convection in the minimal flow unit and to show if a turbulent flow in a domain smaller than that of JM can be sustained. Finally, results of LES are compared with those of DNS of turbulent mixed convection.

2 Governing Equations and Numerical Method

2.1 Direct Numerical Simulations

The finite volume method solves the time-dependent, incompressible governing equations based on the Boussinesq approximation. They read:

$$\frac{\partial u_i}{\partial x_i} = 0 \tag{1}$$

$$\frac{\partial u_i}{\partial t} + \frac{\partial}{\partial x_j}(u_j u_i) = -\frac{1}{\rho}\frac{\partial p}{\partial x_i} + \nu \frac{\partial^2 u_i}{\partial x_j \partial x_j} + \alpha(T - T_m) g_i \delta_{i2} + F\delta_{i1} \tag{2}$$

$$\frac{\partial T}{\partial t} + \frac{\partial}{\partial x_j}(u_j T) = \kappa \frac{\partial^2 T}{\partial x_j \partial x_j} \tag{3}$$

For space discretization, second-order central differencing is used for all terms. The second-order implicit Crank-Nicolson scheme is used for time discretization. The discretized pressure and velocity fields are coupled with a PISO algorithm [9]. A sketch of the minimal flow unit and the coordinate system is illustrated in Fig. 1.

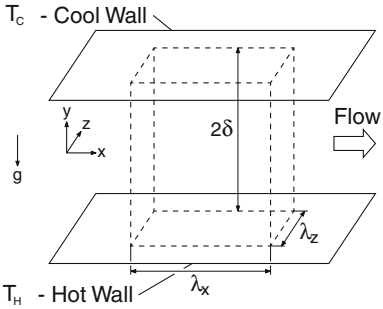

Fig. 1 Geometry of the computational domain with periodic boundary conditions in x- and z-direction

The boundary conditions in both the stream- and spanwise directions are periodic, while top and bottom boundaries are physical walls with no-slip and impermeability conditions. Additionally, the walls temperature is prescribed values $T_H = 274.9\,\mathrm{K}$ and $T_C = 271.4\,\mathrm{K}$, respectively. Throughout this chapter we will use the thermodynamic properties of air for all fluid simulations, i. e. the kinematic viscosity $\nu = 1.35\mathrm{e}-5\,\mathrm{m}^2/\mathrm{s}$, the thermal diffusivity $\kappa = 1.898\mathrm{e}-5\,\mathrm{m}^2/\mathrm{s}$, the density $\rho = 1.276\,\mathrm{kg}/\mathrm{m}^3$ and the thermal expansion coefficient $\alpha = 3.674\mathrm{e}-3\,\mathrm{K}^{-1}$. The buoyancy force acts in wall-normal direction, as well as the gravitational acceleration g. In order to maintain a constant volume flux in the channel flow, we use a forcing function F in the x-direction in the momentum equations. It represents a streamwise mean pressure gradient that needs to be updated at each time step to maintain a prescribed volume flux. The Reynolds number characterising the flow is $Re = u_m\delta/\nu = 2000$ according to JM, where $\delta = 0.18\,\mathrm{m}$ is the channel half width and u_m the volume averaged velocity. Thus, for the Grashof number $Gr = \alpha g\delta^3\Delta T/\nu^2 = 4e^6$, we get an Archimedes number of $Ar = Gr/Re^2 = 1$. As a result of the additionally acting buoyancy force, the wall shear stress is different on both walls. Thus, the friction velocity $u_\tau = \sqrt{\tau_w/\rho}$ and the friction Reynolds number $Re_\tau = u_\tau\delta/\nu$ are the averaged values of the hot and cold wall. In order to define the computational grid, we used the empirical approximation of Pope [10] to predict the friction Reynolds number $Re_\tau = 0.09\,(2\,Re)^{0.88}$. The calculated value of $Re_\tau = 133$ applies to an isothermal simulation. For the simulations of mixed convection the resulting friction Reynolds number is expected to be higher. Therefore, for these simulations we used a even finer grid with a spatial resolution of $\Delta x^+ = 4$ and $\Delta z^+ = 2$ in streamwise and spanwise directions, respectively. The grid is refined in the wall-normal direction, such that the first node at the wall is located at $y_w^+ = 0.1$ and the central spacing is $\Delta y_c^+ = 2.5$. Here, the "+" superscript denotes wall units $\Delta x_i^+ = u_\tau\Delta x_i/\nu$. The physical domain size ($L_x \times L_y \times L_z$) was set to $\pi\ \delta \times 2\,\delta \times \delta$ with a $108 \times 136 \times 68$ grid. As initial condition, we used an instantaneous flow field produced in a DNS of a fully developed turbulent flow of a "full" channel. Before statistical averaging was started, all simulations were processed until no remarkable change in general flow behaviour and the low-order statistical moments was observed. Additionally, we simulated a isothermal turbulent

channel flow in the minimal box of JM to analyse the predictive capabilities of the used finite volume method. For the latter simulation, the momentum Eq. (2) were decoupled from the energy Eq. (3) by setting the buoyancy term to zero.

2.2 Large Eddy Simulations

The following governing equations for the LES are formally obtained by tophat-filtering Eqs. (1)–(3) using a filter width which corresponds to the grid spacing of the coarser LES grid.

$$\frac{\partial \widetilde{u}_i}{\partial x_i} = 0 \tag{4}$$

$$\frac{\partial \widetilde{u}_i}{\partial t} + \frac{\partial}{\partial x_j}(\widetilde{u}_j \widetilde{u}_i) = -\frac{1}{\rho}\frac{\partial \widetilde{p}}{\partial x_i} - \frac{\partial \tau_{ij}}{\partial x_j} + \nu \frac{\partial^2 \widetilde{u}_i}{\partial x_j \partial x_j} + \alpha(\widetilde{T} - T_m) g_i \delta_{i2} + F \delta_{i1} \tag{5}$$

$$\frac{\partial \widetilde{T}}{\partial t} + \frac{\partial}{\partial x_j}(\widetilde{u}_j \widetilde{T}) = -\frac{\partial h_j}{\partial x_j} + \kappa \frac{\partial^2 \widetilde{T}}{\partial x_j \partial x_j} \tag{6}$$

where $\tau_{ij} = \widetilde{u_i u_j} - \widetilde{u}_i \widetilde{u}_j$ and $h_j = \widetilde{u_j T} - \widetilde{u}_j \widetilde{T}$ are the subgrid-scale (SGS) stress tensor and the subgrid-scale heat flux (HF) vector, respectively. These two terms take into account the effect of SGS turbulence and need to be modelled to close the system of governing equations.

We used the dynamic process introduced by Germano [11] and Lilly [12], together with Smagorinsky model [13]. The dynamic Smagorinsky model is known for its features of self-calibration, is free from empirical constants and artificial near-wall damping functions and allows for some backscattering of turbulent kinetic energy from the subgrid-scales to the grid scales. It models the trace-free SGS stress tensor with a function of the resolved strain rate tensor $\widetilde{S}_{ij}$: $\tau_{ij} - \tau_{kk}/3\ \delta_{ij} = -2C_S \widetilde{\Delta}^2 |\widetilde{S}| \widetilde{S}_{ij}$ where $\widetilde{S}_{ij} = (\partial \widetilde{u}_i/\partial x_j + \partial \widetilde{u}_j/\partial x_i)/2$, $|\widetilde{S}| = (2\widetilde{S}_{ij}\widetilde{S}_{ij})^{0.5}$ and $\widetilde{\Delta}$ is the filter width. Following the procedure of [12] we minimize the residual of the Germano identity and obtain $C_S = -(M_{ij}L_{ij})/(M_{ij}M_{ij})$. This equation introduces the resolved Leonard type stress $L_{ij} = \langle \widetilde{u}_i \widetilde{u}_j \rangle - \langle \widetilde{u}_i \rangle \langle \widetilde{u}_j \rangle$ and a differential tensor $M_{ij} = \alpha_{ij} - \widetilde{\beta_{ij}}$ with $\alpha_{ij} = 2\langle \widetilde{\Delta} \rangle^2 |\langle \widetilde{S} \rangle| \langle \widetilde{S} \rangle_{ij}$ and $\beta_{ij} = 2\widetilde{\Delta}^2 |\widetilde{S}| \widetilde{S}_{ij}$. The dynamic model relies on two different filtering operations based on which the model coefficient C_S can be determined. The finer filter is the implicit grid filter ($\sim$) and the coarser filter is the so called test-grid filter ($<>$). In order to avoid negative values for C_S, we applied spatial plane and time averaging of the model coefficient C_S. The dynamic HF model is based on the eddy thermal diffusivity concept in analogy to Fourier's law and was introduced by [14]. It reads: $h_j = -\kappa_t\ \partial \widetilde{T}/\partial x_j = -\nu_t/Pr_t\ \partial \widetilde{T}/\partial x_j = -Pr_t^{-1} C_S \widetilde{\Delta}^2 |\widetilde{S}| \partial \widetilde{T}/\partial x_j$. Here, the SGS eddy thermal diffusivity is κ_t, the SGS eddy viscosity is ν_t and the SGS Prandtl number is the fixed value $Pr_t = 0.5$ as proposed by [14]. The LES was performed on a coarser grid, with $21 \times 88 \times 13$ points in

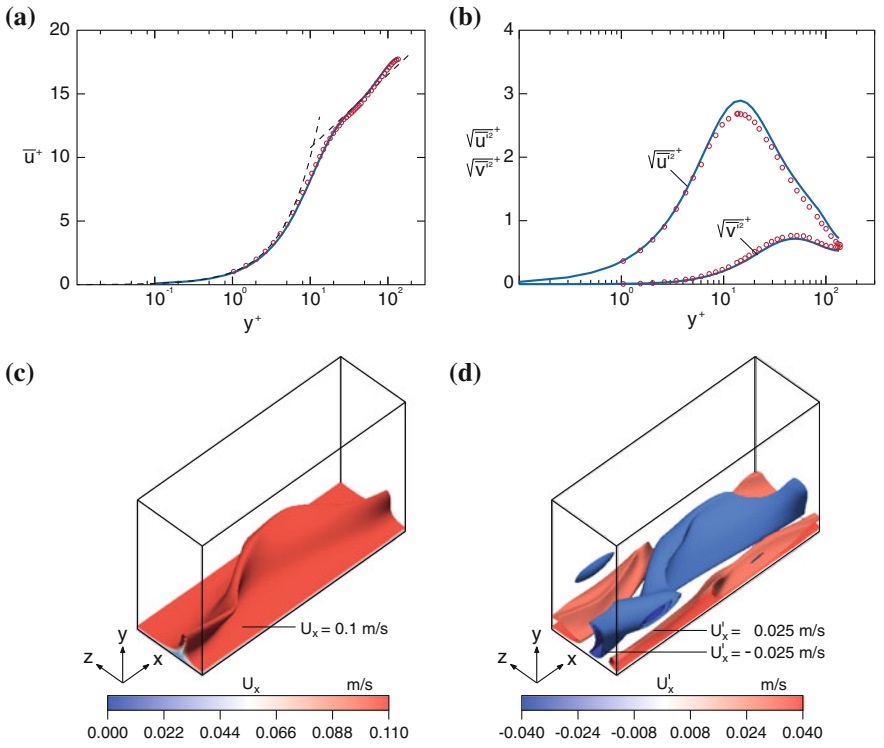

Fig. 2 **a** Mean velocity profile in wall coordinates: DNS (*blue line*) and JM (*red circles*). **b** Root-mean-square (rms) velocity fluctuations in wall coordinates: DNS (*blue line*) and JM (*red circles*). Isosurfaces of instantaneous streamwise velocity component **c** ($u_x = 0.1\,\mathrm{m/s}$) and streamwise velocity fluctuations **d** ($u'_x = 0.025\,\mathrm{m/s}$ and $u'_x = -0.025\,\mathrm{m/s}$)

the x-, y- and z-directions, respectively. Since the domain size was maintained the realized spatial resolution is $\Delta x^+ = 30$, $\Delta z^+ = 15$, $y_w^+ = 0.5$ and $\Delta y_c^+ = 15$, respectively.

3 Results

3.1 DNS of Isothermal Channel Flow

In order to demonstrate the reliability and of the applied second-order accurate finite-volume method used, we simulated turbulent isothermal channel flow in the minimal flow unit of JM. The generated mean streamwise velocity and turbulence intensities profiles in wall coordinates are presented in Fig. 2. Note that the quantities with the $(+)$ superscript are normalized with the friction velocity u_τ. In Fig. 2a, the mean

velocity profile agrees well with the JM data. Furthermore, the profiles of the rms velocity fluctuations shown in Fig. 2b are in good agreement with the JM data as well. There are only small discrepancies in the rms value of the streamwise velocity component in the buffer layer. To demonstrate that the coherent structure discussed above is obtained in the considered minimal flow unit, we illustrated such a structure with isosurfaces of the instantaneous velocity field obtained for some time step in Fig. 2c. We observe one single low-speed streak in the minimal flow unit, which organizes the production of turbulence. The field of velocity fluctuations which is computed by subtracting the mean streamwise velocity component from the instantaneous field shown Fig. 2c is visualized in Fig. 2d. It can be seen that the low-speed streak is surrounded by streaks of high-speed fluid.

3.2 DNS of Mixed Convection

As mentioned above a higher wall shear stress is obtained for turbulent mixed convection. This leads to a increased friction Reynolds number $Re_\tau = 191$. Thus the realized spatial resolution in wall units of the DNS of mixed convection reduces to $\Delta x^+ = 5.7$, $\Delta z^+ = 2.9$, $y_w^+ = 0.14$ and $\Delta y_c^+ = 3.6$, respectively. The predicted mean streamwise velocity, shown in Fig. 3a, agrees well with the law of the wall in the viscous sublayer. Though, farther away from the wall the streamwise velocity values are lower due to the higher turbulence intensity obtained for mixed convection as shown in Fig. 3b. Contrary to the isothermal case, the wall-normal velocity fluctuations are much higher far away from the wall. The corresponding mean temperature profile and the rms temperature fluctuations are presented in Fig. 3c and d, respectively. These graphs show that a turbulent thermal boundary layer develops close to the wall where the mean temperature values $\overline{\theta} = (\overline{T} - T_m)/\Delta T$ significantly deviate from the center temperature $T_m = (T_H + T_C)/2$ as the peaks in the rms temperature fluctuations reveal. In the middle of the channel the rms temperature fluctuations decrease to a minimum. In order to demonstrate that the size of the coherent structures has reduced due to the increased wall shear stress, isosurfaces of the streamwise velocity are presented in Fig. 4a and b. Note, that the scales of Fig. 4a and b are the same as the one of Fig. 2c and d, respectively. The comparison reveals that smaller scales develop for mixed convection which underlines the enhancing effect of buoyancy. In this respect the streaks became thinner and shorter than the single streak observed for the isothermal case. We also performed a number of additional DNS of turbulent mixed convection for which we successively reduced the size of the spanwise width of the domain. The result was that we obtained a turbulent channel flow up to a spanwise width $\lambda_z^+ = 38.2$ (i. e. $L_z = 0.2\delta$).

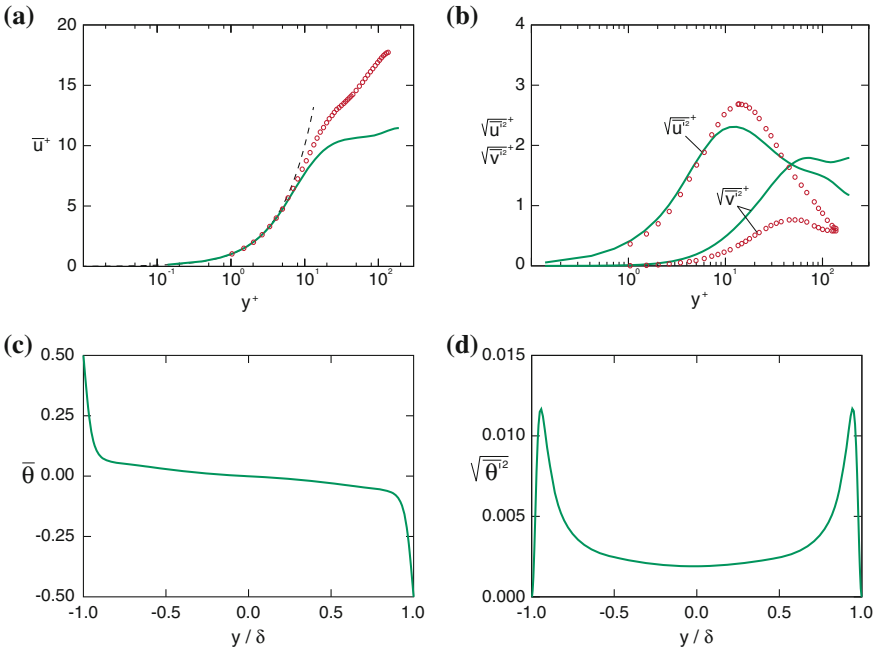

Fig. 3 **a** Mean velocity profile in wall coordinates: mixed (*green line*) and JM (*red circles*). **b** Mean turbulent rms velocity fluctuations in wall coordinates (*green line*) and JM (*red circles*). **c** The normalized mean temperature profile in global coordinates. **d** Mean turbulent rms temperature fluctuations in global coordinates

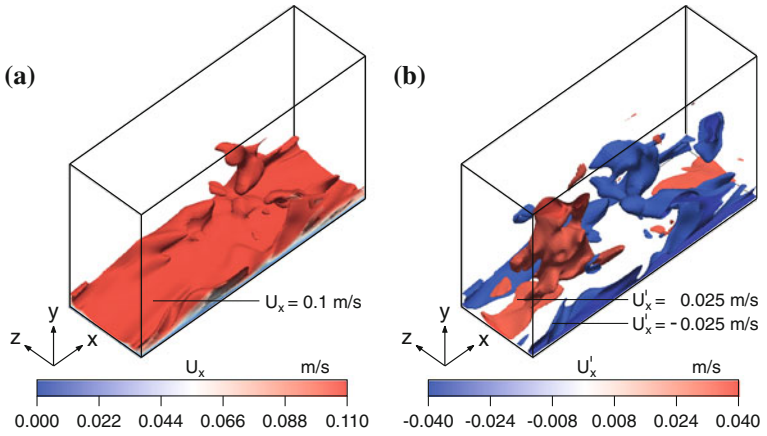

Fig. 4 Coherent structures in mixed convection visualized using isosurfaces of the instantaneous streamwise velocity component in **a** ($u_x = 0.1\,\mathrm{m/s}$) and the streamwise velocity fluctuations in **b** ($u'_x = 0.025\,\mathrm{m/s}$ and $u'_x = -0.025\,\mathrm{m/s}$)

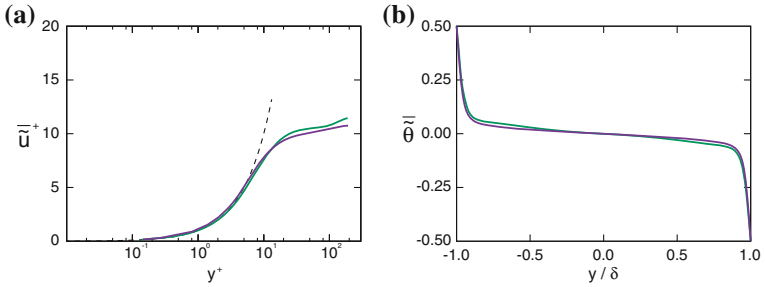

Fig. 5 **a** Mean velocity profile in wall coordinates: DNS (*green line*) and LES (*violet line*). **b** The normalized mean temperature profile in global coordinates: DNS (*green line*) and LES (*violet line*)

3.3 LES of Mixed Convection

The results of the LES are illustrated in Fig. 5a and b. The mean streamwise velocity profile in Fig. 5a matches the DNS data quite well, but it slightly underpredicts the velocity in the region far away from the wall. Fig. 5b additionally shows the normalized temperature profile, which is underpredicted by the LES at the hot wall and overpredicted at the cold wall. Nevertheless, the LES data obtained are in good agreement with the DNS data.

4 Summary

In order to show that the finite-volume method, we used, is accurate enough, we performed a DNS of a turbulent flow in the minimal flow unit for an isothermal case. The spatial resolution realized in this DNS was shown to be fine enough to resolve all relevant turbulent scales. This was confirmed since the DNS results are in good agreement with the reference data by JM. Furthermore, we have also identified similar coherent structures in the minimal flow unit. Since buoyancy increases the wall shear stress, we performed a DNS of turbulent mixed convection. Analysing the results we showed that the streaks became thinner and shorter than in the isothermal case. The analysis of the mean flow field and rms velocity and temperature fluctuations further revealed that buoyancy significantly enhances the production of turbulence. Consequently, we performed additional DNS of turbulent mixed convection for which we successively reduced the size of the spanwise width of the domain and still obtained a self-sustaining turbulent flow. Finally, we conducted a LES of mixed convection with the dynamic Smagorinsky model with spatial plane and time averaging of the model coefficient. The comparison of DNS and LES results revealed that the mean quantities are in good agreement.

References

1. Cantwell, B.J.: Organized motion in turbulent flow. Annu. Rev. Fluid Mech. **13**, 437–515 (1981)
2. Robinson, S.K.: Coherent motions in the turbulent boundary layer. Annu. Rev. Fluid Mech. **23**, 601–639 (1991)
3. Jiménez, J.: Cascades in wall-bounded turbulence. Annu. Rev. Fluid Mech. **44**, 27–45 (2012)
4. Kim, J., Moin, P., Moser, R.: Turbulence statistics in fully developed channel flow at low Reynolds number. J. Fluid Mech. **177**, 133–166 (1987)
5. Jiménez, J., Moin, P.: The minimal flow unit in near-wall turbulence. J. Fluid Mech. **225**, 221–240 (1991)
6. Dean, R.B.: Reynolds number dependence of skin friction and other bulk flow variables in two-dimensional rectangular duct flow. J. Fluids Eng. **100**, 215–223 (1978)
7. Kasagi, N., Nishimura, M.: Direct numerical simulation of combined forced and natural turbulent convection in a verticqal plane channel. Int. J. Heat Fluid Flow **18**, 88–99 (1997)
8. Davidson, L., Čuturić, D., Peng, S.-H.: DNS in a plane vertical channel with and without buoyancy. In: Hanjalić, K., Nagano, Y., Tummers, M.J. (eds.) Turbulence Heat and Mass Transfer, pp. 401–408. Begell House, New York (2003)
9. Issa, R.I.: Solution of the implicitly discretised fluid flow equations by operator-splitting. J. Comput. Phys. **62**, 40–65 (1986)
10. Pope, S.B.: Turbulent Flows, p. 279. Cambridge University Press, Cambridge (2000)
11. Germano, M., Piomelli, U., Moin, P., Cabot, W.H.: A dynamic subgrid-scale eddy viscosity model. Phys. Fluids A **3**, 1760–1765 (1991)
12. Lilly, D.K.: A proposed modifications of the Germano subgrid-scale closure method. Phys. Fluids A **4**, 633–635 (1992)
13. Smagorinsky, J.: General circulation experiments with the primitive equations. Mon. Wea. Rev. **91**, 99–164 (1963)
14. Moin, P., Squires, K., Cabot, W., Lee, S.: A dynamic subgrid-scale model for compressible turbulence and scalar transport. Phys. Fluids A **3**, 2746–2757 (1991)